ANALYSIS OF A FERROMANGANESE SECONDARY FUME EXTRACTION SYSTEM TO IMPROVE DESIGN METHODOLOGIES

[1]Luther Els, [2]Peter Cowx, [2]Roy Nordhagen, [3]Gerrit Kornelius, [4]Nicole Andrew, [5]Patrick Smith

[1] Resonant Environmental Technologies, Pretoria, South Africa, e-mail: luther@resonant.co.za
[2] Eramet Norway, Sauda, Norway, e-mail: roy.nordhagen@erametgroup.com
[3] University of Pretoria, Pretoria, South Africa, e-mail: gerrit.kornelius@up.ac.za
[4] Resonant Environmental Technologies, Pretoria, South Africa, e-mail: nicole@resonant.co.za
[5] Resonant Environmental Technologies, Pretoria, South Africa, e-mail: patrick@resonant.co.za

ABSTRACT

Hot metal handling operations at smelters generate a significant amount of fume. The effective management and removal of these fumes is important to keep in line with environmental legislation as well as to improve working conditions on site.

The available literature gives standard design methods for fume extraction hoods based on the assumption that the volume and velocity of the fume can be calculated from natural convection above a hot surface. This paper considers the validity of this assumption and investigates the relationship between the theory and actual data from a functioning extraction system. Other fume generation methods investigated were radiation, chemical reactions and taphole emissions.

An extensive test campaign on an existing secondary fume extraction system at Eramet Norway, Sauda was used as the basis for the study. The MOR sand bed extraction hoods were determined to be underperforming therefore various improved extraction options were modelled using CFD. Verification runs were performed to analyse the energy generation mechanisms. These results were compared to site testing data to verify the energy flux and then the results were checked with the video analysis. Various meshes were considered to compare plume growth and a transient run was also performed. Once the input parameters and meshing were verified, numerous hood configurations were modelled and compared.

KEYWORDS: *Secondary fume, manganese, tapping, extraction, design, hoods.*

Eramet Sauda operates two ferromanganese furnaces as well as a Manganese Oxygen Refining (MOR) unit. Secondary fume emissions are generated at the tap holes as well as post-taphole operations. The existing secondary fume capture system has good capacity, but fugitive emissions from the furnace building do occur and a study is required to optimise and upgrade the capture system. The manganese oxides present in these fumes are easily inhaled due to their small size. Health effects include the contraction of manganism, a serious (and irreversible) brain disease, and various lung disorders. The American Conference of Governmental Industrial Hygienists (ACGIH) recommends a TLV of 0.2 mg/m^3 TWA for Manganese and Manganese oxides. Norwegian laws for respirable manganese dust have become more stringent since 2008-07-01 and must be within a limit of 0.1 mg/m^3 as an 8 hour average [1, 2].

2. THEORETICAL BACKGROUND

2.1. NATURAL CONVECTION

The majority of fume extraction systems are designed based on flow rates calculated from thermal updrafts, or plumes, caused by convective heat transfer from the hot surface concerned [3]. The convective heat transfer rate is calculated using equation [4].

$$\Phi = hA_s(T_s - T_\infty) \quad (1)$$

Where h is the convective heat transfer coefficient, A_s is the surface area of the hot metal surface, T_s is the surface temperature and T_∞ is the temperature of the surrounding air (Cengel & Ghajar, Heat and Mass Transfer, 4th Edition, 2011). Many different correlations exist for the calculation of the heat transfer coefficient, which is a function of the geometry of the surface concerned and the flow regime of the fluid concerned.

The flow rate, $q_{v,z}$, and centre line velocity, ν_z, of the convective plume are calculated as follows (Where z is the height above the point source) [5]:

$$q_{v,z} = 0.005\Phi^{1/3}z^{5/3} \quad ; \quad \nu_z = 0.128\Phi^{1/3}z^{-1/3} \quad (2)\ (3)$$

2.2. REACTION ENERGY

2.2.1. Mechanisms

Mn_3O_4 has the highest Gibbs free energy of formation of the manganese oxides, making it the most likely product to form. This conclusion was verified by a chemical analysis of the MOR baghouse dust which showed a 97 % Mn_3O_4 composition.

Gonser and Hogan [6] describe various mechanisms of fume generation from a hot metal surface during welding that can be applicable to ferroalloy fume generation. Due to the high metal temperatures in ferromanganese processing, evaporation followed by oxidation of the vapour directly into the solid oxide state is considered to be the most significant mechanism of fume generation. It is assumed that the energy required for evaporation is derived from the metal and contributes to a lowering in the metal temperature [7].

2.2.2. Oxidation Enhanced Vapourisation

The maximum possible rate of vapourisation occurs in a vacuum and is calculated using the Langmuir equation which is derived from the kinetic theory of gases [8, 9]:

$$E_{Mn} = p_{Mn}\left(\frac{M_A}{2\pi RT}\right)^{0.5} \quad (4)$$

Where E_A is the evaporation rate of A in kg/s.m^2, M_A is the molar mass of A in kg/gmol and R is the universal gas constant in J/gmol.K. Turkdogan et al. [9] have shown that, in high oxygen atmospheres, metal evaporation rates can approach that predicted by the Langmuir equation. This effect is known as oxidation enhanced vapourisation and is caused by oxidation of the metal vapour above the liquid surface [10].

2 .2.3. Mass Transfer Limited Vapourisation

In reality, oxygen concentrations may not be high enough to cause oxygen enhanced vapourisation, especially at high temperatures where the volatility of the manganese is high. Lee and Kolbeinsen [11] suggested that manganese vapour does not oxidise when the partial pressure of oxygen is less than 17 kPa. At atmospheric oxygen concentrations and high metal temperatures the manganese evaporation is limited by the mass transfer of manganese through a diffusion boundary layer above the metal surface as given by:

$$J_{Mn} = \frac{h_{Mn}}{RT}\left(P_{Mn}{}^{sat} - p_{Mn}\right) \quad (5)$$

Where J_{Mn} is the evaporation flux of the manganese in mol/m^2.s, $h_{Mn} = D_{Mn}/l$ is the average mass transfer coefficient of the manganese vapour and p_{Mn} is the partial pressure of manganese at the top of the mass transfer boundary layer, *l*.

The saturation pressure of manganese above a Mn-Fe-C system, as is the case for a ferromanganese melt, can be determined from Raoult's law which accounts for the non-ideality of the melt. Lee [12] determined an equation for the activity coefficient of manganese in a Mn-Fe-C system using the Unified Interaction Parameter Model.

2 .2.4. Summary

The energy generated from the oxidation of evaporated manganese to Mn_3O_4 can be assumed contribute to the plume energy. The oxidation rate can be assumed to be proportional to the rate of manganese evaporation above oxygen partial pressures of 17 kPa. The evaporation rate is limited by the mass transfer of manganese away from the metal surface, which may be enhanced by oxidation at higher oxygen concentrations.

2.3. RADIATION

Energy transferred as radiation from any surface is calculated as follows:

$$Q = \sigma \varepsilon A_s (T_s{}^4) \quad (6)$$

Where σ is the Stefan-Boltzmann constant (5.67x10^{-8} W/(m^{2}K^4)), ε is the emissivity of the surface concerned, A_s is the surface area and T_s is the temperature of the surface (Cengel & Ghajar, Heat and Mass Transfer, 4th Edition, 2011) [13].

Due to the high metal temperatures during tapping and subsequent operations, the amount of energy released from the metal surface in the form of radiation is very high, in the order of 100 to 300 kW/m^2, depending on the metal surface temperature and emissivity.

Non-polar gases such as O_2 and N_2 are essentially transparent to radiation. Polar molecules, such as CO_2 and water vapour, are capable of absorbing radiation (Cengel & Ghajar, Heat and Mass Transfer, 4th Edition, 2011) [13]. These gases are estimated to be in very low concentrations in the fume plume and therefore radiation is not expected to contribute directly to plume growth in this manner.

The presence of metal oxides and other particulates within fumes have a significant effect on radiation heat transfer (Cengel & Ghajar, Heat and Mass Transfer, 4th Edition, 2011) [13]. The

particulates may cause a large proportion of the incident radiation to be reflected, thereby reducing the energy transmitted, and possibly absorbed by the surrounding gas. The particles themselves may also emit small amounts of thermal radiation. The particle effects are difficult to quantify. Particle size distributions, concentration and surface emissivities are required, which are not available at this stage. Particle radiation effects were therefore not taken into account in this study.

2.4. TAPHOLE EMISSIONS

Depending on furnace operating conditions, a significant amount of fume can be released from the furnace through the taphole. The amount of fume released is highly variable and depends on a number of factors including the pressure inside the furnace and conditions during tapping (6). Due to the highly inconsistent nature of this fume source it cannot be modelled for the average case and a range of taphole emission rates should be considered to ensure a robust taphole extraction design.

3. TEST RESULTS

3.1. FLOW TESTING

Sauda has a dedicated emission system baghouse, the Environmental filter, with three fans. The system is designed to extract from one point per fan at one time. An extensive test campaign was carried out at Sauda on the existing fume extraction system. The flow and energy were logged continuously at the extraction fan inlet and tests were performed close to the hoods during the various operations. The results of relevant extraction hoods are shown in table 1.

Table 1: Summary of extraction system test results

Test Point	Velocity	Temp-erature	Static Pressure	Volume Flow		Mass Flow	Energy
	m/s	°C	kPa	Am3/s	Nm3/h	kg/s	MW
Furnace 11 fan	21.1	36.4	-2.57	47.9	147235	54.4	
F11 - Casting Bed 4	28.3	27.6	-3.29	37.5	118648	43.9	1.2
F11 - Casting Bed A	36.8	27.6	-2.94	48.8	154911	57.0	2.8
MOR Fan	36.5	20.1	-3.57	48.5	156861	58.1	
LCFeMn Pour Point	32.6	35.8	-2.57	43.3	134513	49.3	2.5

An ambient temperature of 20°C as measured on site was used as the reference temperature for all energy calculations. A combination of traverses and continuous monitoring at the extraction points and continuous monitoring at the fans was used to determine the maximum energy values.

The fume capture was observed to be good in most areas, except when more than one extraction point was in use per fan. One area of concern, however, is the MOR Sand Beds. This area is used for casting of the LCFeMn from the converter. There are two longitudinal beds, back to back with a common pour point. There is an extraction point above the pour point, which is served by the Environmental Filter, and a hood over the first few bays of each of the beds, which is served by the MOR filter.

The energy captured by the secondary fume system is much higher for the Group A sand beds than for Sand Bed 4. This is because at Sand Bed 4 the extraction point is only over the pour point and the rest of the fume is not captured. For the Group A bed, where the entire area is enclosed,

almost twice the energy is captured. The energy captured at the MOR sand bed pour point was 2.5 MW, as compared to 1.2 MW from the HCFeMn pour point at Sand Bed 4. This is in line with the theory, as the LCFeMn is at a higher temperature after the converter than the HCFeMn. Because there is no effective extraction installed at the MOR Sand Beds, the energy could not be measured. Based on the energy comparisons of pour point versus bed and HCFeMn versus LCFeMn, the energy is the MOR sand bed plume was estimated to be in the range of 3 to 4 MW.

3.2. VIDEO ANALYSIS

Video analysis was performed at the MOR low carbon casting sand beds, where the fume generation was of the most concern. A grid was set up over the video and the height of the grid blocks was calculated according to a measured scaling factor. The video was moved forward frame by frame and the time taken for the fume to rise through one grid section was measured. From this the velocity was calculated. Numerous measurements were taken and averages obtained. For design purposes the maximum fume emissions are of concern. There was no clear trend towards higher velocities in a particular area. The overall average velocity measured was 0.9 m/s with a 0.4 m/s standard deviation. The maximum velocity measured was 1.4 m/s.

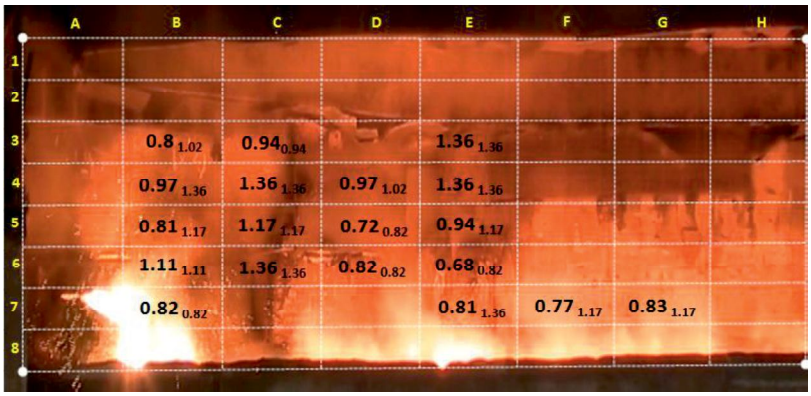

Figure 1: MOR casting at Sand Bed 3 with the average velocities for each grid sector in bold and the maximum values below, in m/s

4. CFD MODELLING

CFD modelling was used to simulate the fume rising off the sand bed and evaluate the capture efficiency of various hood designs. The simulations were run using FloEFD 11.3.0.

Initially a validation model was set up to compare the CFD results to the measurements taken on site. A meshing study was performed using this model. A number of limitations were identified with the modelling technique used but it was found that the chosen method resulted in conservative evaluation of the performance of the various hood designs. The sensitivity of the most practical solution was evaluated against increased emissions.

The modelling limitations were a result of the computational resources available and the time restraints imposed on the project. The limitations are listed below:

- The level of mesh refinement was limited to between 1 million and 2 million cells. This was done to minimise the run time while still getting meaningful results.
- FloEFD only utilises a kε turbulence model. This model is based on a 2D vortex assumption. The turbulence in this case is 3D. A more advanced turbulence model such as full stress Reynolds would provide a better simulation of the flow development.

- A steady-state formulation has been used. Heat convection is inherently unsteady. While it was possible to use an unsteady formulation, during the verification process is was concluded that the steady state formulation would give satisfactory results to make a conservative evaluation the capture efficiencies of the hoods.
- The video analysis used in the verification only analyses the outside of the plume. Using a technique such as Planar Particle Image Velocimetry the velocity of the particles within the plume could be recorded. This type of equipment was not available at the time of the testing.

4.1. CFD VERIFICATION WITH TEST RESULTS AND THEORY

An initial model was created to quantify the heat transfer due to the convection from the metal plates and the radiation received by the wall. For these calculations the following metal surface temperatures were applied to the plates:

Table 2: Metal temperature used in initial heat transfer simulation

Region	Temperature, °C
Plates 1-4	1650
Plates 5-7	1550
Plates 8-10	1500

The total heat transfer was found to be significantly lower than the energy measured on site. This supports the assumption that the reaction energy contributes to the plume growth. These values were used as baseline to which additional heat transfer was added.

The upward velocity of the fume was then compared to the velocities measured in the video analysis. It was found that a total input heat transfer rate of 3.4 MW gave the closet result to what was measured on site. This result can be seen if figure 2 is compared to figure 1. The 3.4 MW is also comparable with energies measured on site.

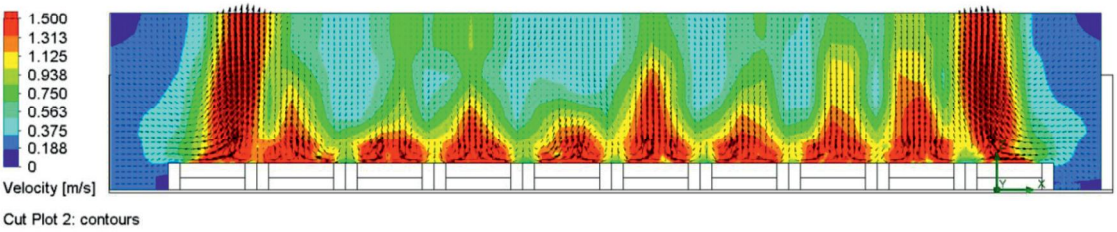

Figure 2: Velocity plot at the outside of plume of the verification model. (Range 0-1.5m/s)

A comparison was made of the results from steady-state and transient simulations using different levels of mesh refinement. While differences were found in the results of these simulations it was concluded that by using a steady-state simulation with Mesh 1 in figure 4, the largest plume would be simulated. This would in turn lead to conservative evaluation of various hood designs. As this configuration would allow the runs to be completed in the practical time frame the hood evaluations were run using these parameters.

4.2. CFD BOUNDARY CONDITIONS

Based on the verification runs, the following fixed heat transfer rates were applied to the metal plates and the wall behind the sand beds for further modelling. The values applied to the

metal plates represent the heat convection from the hot metal and the reaction energy due to the oxidation of the evaporated Mn_2O_3. The value applied to the wall represents the natural convection to the gas from the heated wall surface.

Outlet mass flow boundary conditions were applied to the off takes of the hoods. In practice the distribution of the extraction flow will be controlled by the design of the ducting and the use of balancing dampers. The current extraction from the MOR sand beds is 120 000 Nm^3/hr. This was converted to a mass flow of 42.25 kg/s for use in the CFD analysis.

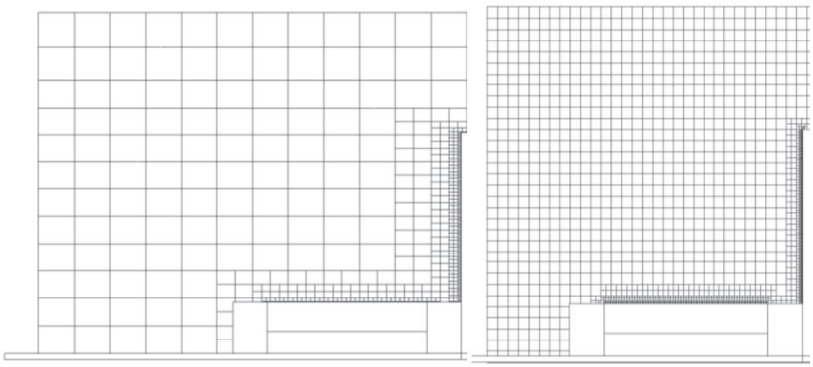

Figure 3: Cut plots through meshes. Left: Mesh 1 Right: Mesh 2

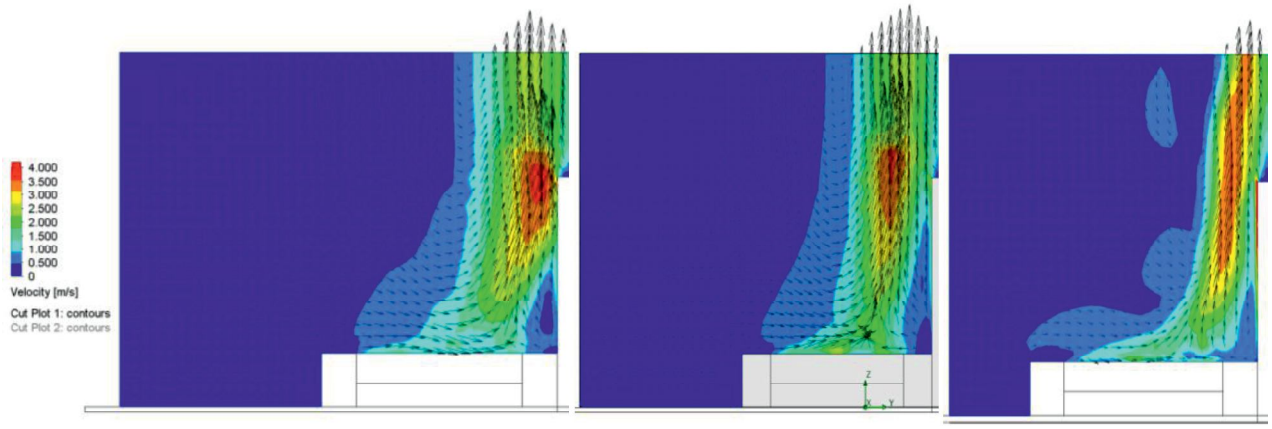

Figure 4: Velocity plot through the middle of a metal plate 3. Left: Mesh 1 Steady-state Middle: Mesh 1 Unsteady Right: Mesh 2 Unsteady (Range: 0-4m/s)

Table 3: Input heat transfer rates

Region	Heat transfer rate	Area	Heat Flux
	kW	m^2	kW/m^2
Plates 1-4	1273	24.64	51.66
Plates 5-7	951.5	18.48	51.48
Plates 8-10	949.8	18.48	51.40
Wall	230.8	60.00	3.85
Total	3405	-	-

In the simulation where double the extraction flow was considered the mass flow was increased to 84.5 kg/s. Doubling the extraction volume was regarded as a practical modification as this could be achieved by installing an additional fan and two additional compartments to the

existing filter. Ten different hood arrangements were considered. The design of the hood itself, height between the bottom of the hood and sand beds and extraction volume were varied.

4.3. CFD RESULTS

The capture efficiency was calculated as the percentage of input heat transfer which was extracted via the hood off takes. The efficiencies of the 10 arrangements are compared in table 4.

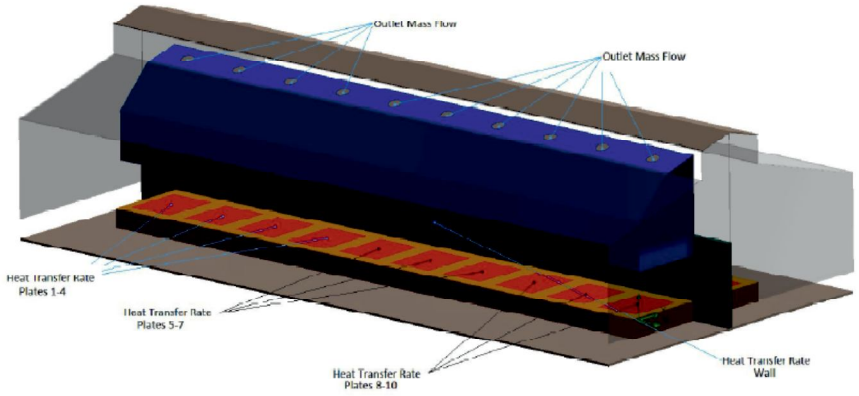

Figure 5: Typical application of boundary conditions

Table 4: Comparison of arrangement capture efficiencies

Run	Hood Design	Height above bed	Extraction rate	Efficiency
		m	kg/s	%
1	Large Hood	2.00	42.25	94
2		1.00	42.25	96
3		0.00	42.25	100
4		2.00	84.50	100
5	Aaberg Hood	0.25	42.25	52
6		0.75	42.25	44
7		0.25	84.50	88
8	Medium Hood	2.00	42.25	91
9		2.00	84.50	100
10	Sliding covers	0.00	42.25	100

The comparison of the capture efficiencies showed that for 100 % capture either the extraction volume must be doubled or the beds be totally enclosed.

Practical concerns of the enclosed arrangements that were raised were the lifespan of the movable parts under the extreme thermal conditions and nuisance of having to replace and remove these parts before and after every tap.

Practically operations would not be hindered by the high overhead hoods, as shown in figure 6. A height of 2.0 m allows enough clearance for the cast plate to be removed by the front end loader. Wind sensitivity could be significant due to the large exposed area above the beds.

To quantify the sensitivity of the double extraction overhead hoods to increases in fume generation additional runs were done using run 4 as a base. The input heat transfer rates of run 4 were increased by 20 %, 40 %, 60 % and 80 % to form runs 11, 12, 13 and 14 respectively.

5. CONCLUSIONS

Natural convection was shown to be a minor contributing factor to the plume energy. The oxidation of evaporated manganese was considered as an additional heat source. The evaporation rate is most likely limited by the mass transfer of manganese through the diffusion boundary layer above the metal surface, but it could be enhanced by oxidation if oxygen concentrations are high enough. Further test work is required in this area.

A combination of site extraction duct testing and video analysis was used to determine suitable CFD input parameters. CFD analyses were performed on 10 different hood arrangements. It was found that to achieve 100 % fume capture either the sand beds need to be totally enclosed by the hood or the extraction volume needs to be increased. A sensitivity analysis on Run 4 (Large hood with double extraction) shows little variation in the capture efficiency until the input heat transfer is increased by 80% from the measured 3.4 MW.

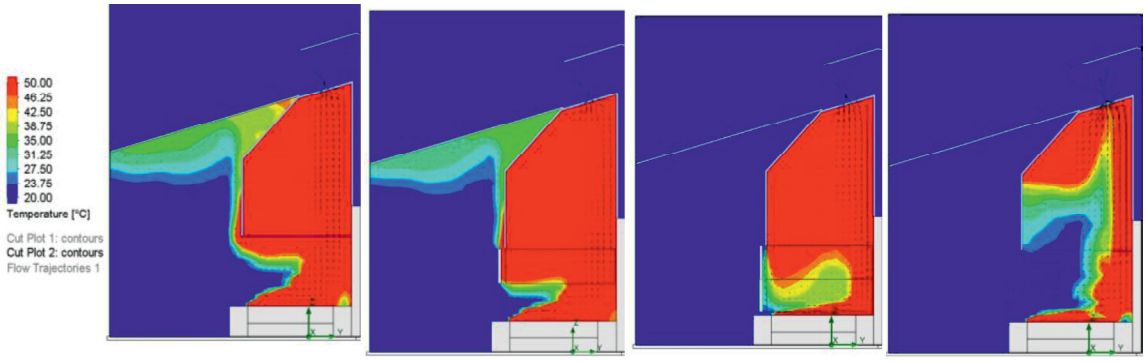

Figure 6: Comparison of temperature plot through plate 3.
From left to right: Run 1, Run 2, Run 3, Run 4. Range (20-50°C)
Temperatures over 20°C outside of the hood volume indicates fume leakage

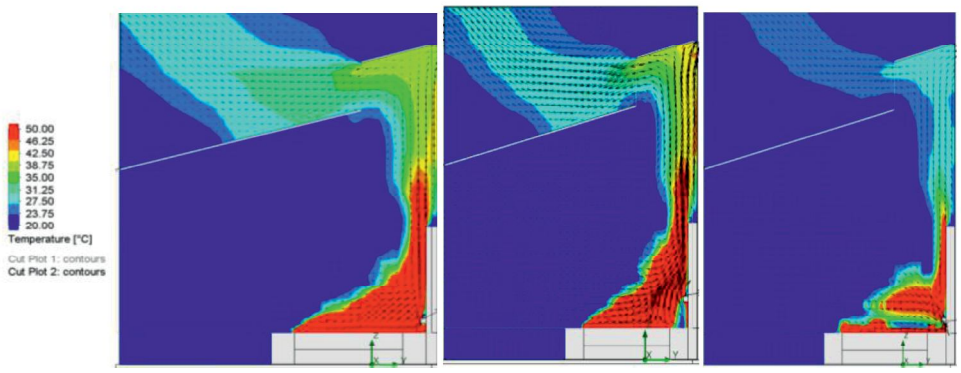

Figure 7: Comparison of temperature plot through plate 3. From left to right: run 5, run 6, run 7.
Range (20-50°C) Temperatures over 20°C above of the hood level indicates fume leakage

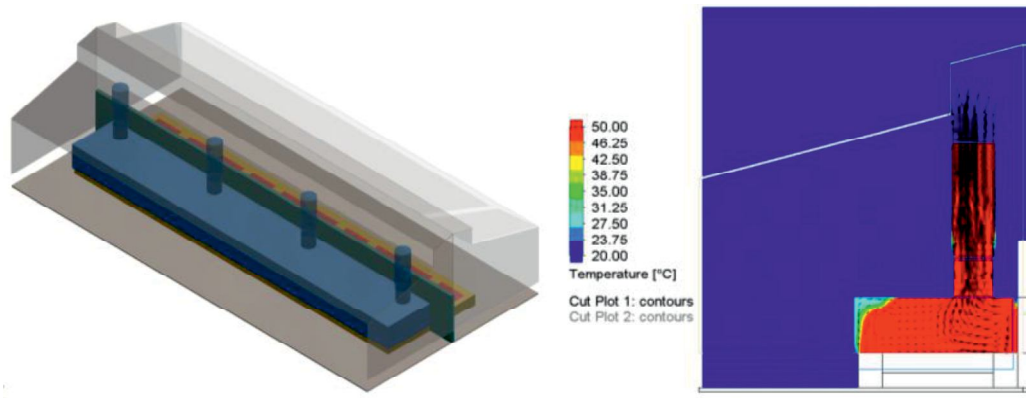

Figure 8: Left: Illustration of Run 10 (sliding cover concept).
Right: Temperature plot through plate 4 (Range 20-50°C)
Temperatures over 20°C outside of the hood volume indicates fume leakage

Table 5: Capture efficiencies of sensitivity simulations

Run	Hood Design	Wind	Input heat transfer rate	Height above bed	Extraction rate	Efficiency
		m/s	MW	m	kg/s	%
11	**Large Hood**	0	4.1	2.00	84.5	100
12		0	4.8	2.00	84.5	99
13		0	5.4	2.00	84.5	98
14		0	6.1	2.00	84.5	91

6. REFERENCES

[1] Arbeidstilsynet. Arbeidsmiljøloven – administrative normer for forutrensning. 7439-96-5.
[2] Institute, International Manganese. Regulatory Limits for Mn and Mn Compounds. s.l. : International Manganese Institute. s.1.
[3] Design of Tapping Fume Extraction Systems for Ferroalloy Furnaces. Els, L, Coetzee, C and Vorster, O. Helsinki : Twelfth International Ferroalloy Congress, 2010.
[4] Cengel, YA and Ghajar, AJ. Heat and Masst Transfer, 4th Edition. New York : McGraw Hill, 2011.
[5] Goodfellow, H and Tahti, E. Industrial ventilation Guidebook. California : Academic Press, 2001.
[6] Arc Welding Effects, Fume Formation Mechanisms and Characteristic Methods. Gonser, M and Hogan, T. s.l. : Intech, 2011.
[7] Selective Evaporation of Metals from Weld Pools. Black-Bolten, A and Eager, TW. s.l. : American Society for Metals.
[8] A Model for Prediction of Fume Formation Rate in Gas Metal Arc Welding (GMAW), Globular and Soray Modes, DC Electrode Positive. Dennis, JH, et al., et al. 2, Annals of Occupational Hygiene, Vol. 45, pp. 105-113.
[9] Enhancement of Diffusion-Limited Rates of Vaporization of Metals. Turkdogan, ET, Grieveson, P and Darken, LS. 1963, Journal of Physical Chemistry, Vol. 67, pp. 1647-1654.
[10] Dushman, S. Scientific Foundation of Vacuum Technique. New York : John Wiley and Sons, 1949.

[11] Modest, MF. Radiative Heat Transfer 2nd Edition. 2003.
[12] Silicon Process - New Hood Design for Tapping Gas Collection. Kadkhodabeigi, M, Tveit, H and Berget, KH. Helsinki : Twelfth International Ferroalloys Congress, 2010.
[13] Perry, RH and Green, DW. Perry's Chemical Engoneers Handbook, 8th Edition. New York : McGraw Hill, 2008.
[14] Hultgreen, R, et al., et al. Selected Values of Thermodynamic Properties of Metals and Alloys. New Year : John Wiley and Sons, 1963.